



Provided by the author(s) and University of Galway in accordance with publisher policies. Please cite the published version when available.

Title	Methodical fitting for mathematical models of rubber-like materials
Author(s)	Destrade, Michel; Saccomandi, Giuseppe; Sgura, Ivonne
Publication Date	2017-02-08
Publication Information	Destrade, Michel, Saccomandi, Giuseppe, & Sgura, Ivonne. (2017). Methodical fitting for mathematical models of rubber-like materials. <i>Proceedings of the Royal Society A: Mathematical, Physical and Engineering Science</i> , 473(2198). doi: 10.1098/rspa.2016.0811
Publisher	The Royal Society Publishing
Link to publisher's version	http://dx.doi.org/10.1098/rspa.2016.0811
Item record	http://hdl.handle.net/10379/6482
DOI	http://dx.doi.org/10.1098/rspa.2016.0811

Downloaded 2024-04-19T03:49:11Z

Some rights reserved. For more information, please see the item record link above.



Methodical fitting for mathematical models of rubber-like materials

Michel Destrade¹, Giuseppe Saccomandi^{1,2} and Ivonne Sgura³

¹School of Mathematics, Statistics & Applied Mathematics,
NUI Galway, University Road, Galway, Ireland

²Dipartimento di Ingegneria,
Università degli Studi di Perugia,
Via G. Duranti, Perugia 06125, Italy

³Dipartimento di Matematica e Fisica “E. De Giorgi”,
Università del Salento,
Via per Arnesano, 73100 Lecce, Italy

keywords: nonlinear elasticity, constitutive equations, rubber.

Abstract

A great variety of models can describe the non-linear response of rubber to uni-axial tension. Yet an in-depth understanding of the successive stages of large extension is still lacking. We show that the response can be broken down in three steps, which we delineate by relying on a simple formatting of the data, the so-called Mooney plot transform. First, the small-to-moderate regime, where the polymeric chains unfold easily and the Mooney plot is almost linear. Second, the strain-hardening regime, where blobs of bundled chains unfold to stiffen the response in correspondence to the “upturn” of the Mooney plot. Third, the limiting-chain regime, with a sharp stiffening occurring as the chains extend towards their limit. We provide strain-energy functions with terms accounting for each stage, that (i) give an accurate local and then global fitting of the data; (ii) are consistent with weak non-linear elasticity theory; and (iii) can be interpreted in the framework of statistical mechanics. We apply our method to Treloar’s classical experimental data and also to some more recent data. Our

method not only provides models that describe the experimental data with a very low quantitative relative error, but also shows that the theory of non-linear elasticity is much more robust than seemed at first sight. This modelling is also a fundamental advance of computational solid mechanics, because any reliable numerical simulation of a deformation and/or stress field must rely on the choice of a suitable constitutive relation.

1 Introduction

The Mechanics of Rubber-like Solids has a long and prolific history. Following World War II, a huge research effort was launched to find an explicit strain-energy function able to describe accurately the experimental data obtained from the testing of natural and synthetic rubbers. However, in spite of decades of intensive work in that area, to this day there is still no effective model able to perform this task in a satisfying and universal way.

This state of affairs is a plain fact, which cannot be hidden by the countless and seemingly successful models and simulations to be found in the literature. These simulations may be concretely descriptive but in the end, they apply only to some special phenomena. From the point of view of physical sciences, constitutive models must be *universal*, not in the sense that a single model should describe the mechanical behavior of all elastomers, but in the sense that, for a given soft material (e.g. a given sample of natural rubber), a given model should describe its mechanical response in a satisfactory manner for all deformation fields and all stretch ranges physically attainable. Here, a *satisfactory* model is defined as a model able to describe the experimental data first of all from a qualitative point of view and then from a quantitative point with acceptable relative errors of prediction with respect to the data. In the end, it must be kept in mind that a simulation in computational solid mechanics, irrespective of its degree of sophistication, is as good, *or as bad*, as the model it relies upon.

Over the years various mathematical models have been proposed and are now listed in literature reviews, e.g. (Boyce and Arruda 2000, Marckmann and Verron 2006, Beda 2014). By scanning all these constitutive models, we can identify *three fundamental breakthroughs*. First, the Mooney-Rivlin strain energy density (Mooney 1940): a purely phenomenological theory stemming from the early tremendous effort devoted to rewrite the theory of Continuum Mechanics using the language of Tensor Algebra. The Mooney-Rivlin model led to the exploration of the non-linear theory of elasticity in deep and unexpected ways, yielded significative classes of non-homogeneous exact solutions

and provided a new perspective to the interpretation of experimental data.

The second breakthrough has been the Ogden strain-energy density function (Ogden 1984): a rational re-elaboration of the Valanis-Landel hypothesis. For the first time, it became possible to fit accurately theoretical stress-strain curves to experimental data for a variety of deformations and a large range of strains.

The third breakthrough is more complex to describe: it consists in the recent re-elaboration of the ideas underpinning the classical derivation of the neo-Hookean strain-energy based on the basic tools of *statistical mechanics*. Here there are two possible approaches. One is based on micro-mechanical considerations, see for example De Tommasi et al. (2015) for a recent exploration in this direction and the review Puglisi and Saccomandi (2016). The other is based on molecular considerations, see the detailed paper by Rubinstein and Panyukov (2002) on the elasticity of polymer networks for a survey. Below we summarize the micro-mechanical multi-scale approach.

The basic assumption used to derive, from microscopic considerations, the usual models of the mechanical behavior of biological and polymeric networks is the *entropic nature* of their elasticity (Treloar 2005). Because the mechanical response of these materials is due to the deformation of the individual chains or filaments composing the network, there is a strict relationship between the conformations of these macromolecules and the mechanical response of the full macroscopic network. This situation allows for a simple and direct method to determine the macroscopic strain-energy starting from simple mesoscopic considerations. Hence the non-linear force-deformation relationship of an ideal chain is easily obtained by considering that the chain's free energy is purely entropic; then the passage from the single chain model to the full network model is achieved by means of some *phenomenological* average procedures (Treloar 2005).

Indeed, when we model real macromolecules we rely on several idealized assumptions. For example, when we assume that there are no interactions between the monomers composing the molecule, we are considering in fact the mathematical model of an *ideal chain*. It is possible in principle to compute in a careful and detailed way the conformations of such chains in space (Flory 1989), but these computations are cumbersome and usually very complex from a mathematical point of view. For this reason further *ad hoc* approximations for describing the *end-to-end-distance* of a chain are introduced (Rubinstein and Colby 2003).

The most common of these approximations is given by the *Gaussian Chain Model* (Treloar 2005). The output of this approximation is a linear relationship between the applied force magnitude, f , and the average distance between the chain ends, $\langle R \rangle$, along the direction of the applied

force. This approximation is clearly valid in the small force limit, but the non-linear regime calls for more sophisticated approximations. Among the various possibilities, two such non-linear models are very popular: the *Freely Jointed Chain* model (FJC) for polymers and the *Worm-Like Chain* model (WLC) for stiff biological molecules (Rubinstein and Colby 2003).

Both the FJC and the WLC models introduce the concept of *contour length*. The contour length of a polymer chain is its length R_{\max} at the maximum physically possible extension. Because only one configuration can be associated to the maximum extension of the chain in the entropic theory of elasticity, we must have $f \rightarrow \infty$ as $\langle R \rangle \rightarrow R_{\max}$. This requirement cannot be captured by the Gaussian chain model. The main difference between the FJC and the WLC models lies in the divergence behaviour of the force as $\langle R \rangle \rightarrow R_{\max}$. For the FJC model, we have a first-order singularity: $f \sim (\langle R \rangle - R_{\max})^{-1}$ whereas for the WLC model, we have a stronger divergence: $f \sim (\langle R \rangle - R_{\max})^{-2}$.

In between the Gaussian Chain model –early stretch regime– and the FJC or WLC models –late stretch regime– we find a stage of *strain hardening* in tension. For instance Toan and Thirumalai (2010) recently summarised this situation for polymers in a good solvent, where the polymeric chains decompose into a succession of independent *blobs*, so named by Pincus (1976) who proposed a scaling law $f \sim \langle R \rangle^{3/2}$. We emphasize that in general the behavior of the polymeric chain is different from the specific one considered by Pincus but that still, a strong strain hardening effect manifests itself when we go from the small deformation regime to the moderate deformation regime.

Now consider the most basic, but still open, problem of rubber-like mechanics: *a meaningful fitting of experimental simple tension data*. The demand for a model able to describe the entire range of attainable uniaxial tension data is manifest in technological applications of rubber-like materials. There, finite element computations play a fundamental role and almost all commercial codes rely on the tangent modulus method. To be effective, this method needs a model able to capture the *entire* data gleaned from a uniaxial tension test. We propose to rely on the ideas exposed above for a multiscale approach, by following a rational (and reasonable) procedure in the framework of the non-linear theory of elasticity.

In the next section, we recall the tenets of non-linear elasticity theory, with a focus on modelling the mechanical response of an isotropic incompressible hyperelastic material such as rubber. We see that the strain energy density W is a function of two variables only, the first two principal invariants of strain and that a reasonable mathematical candidate for W must at

least be consistent with fourth-order weak non-linear elasticity. For uni-axial data, an historical formatting—the Mooney transform—reveals three distinct regimes of stretch: small-to-moderate, strain-hardening, limiting-chain, which we delineate rigorously. We also show that the fitting procedure should rely on minimising the relative errors as opposed to the classical (absolute) residuals, because it provides the most consistent fitting across all regimes and all measures of stress and strain.

In Section 3 we present two sets of data on the uni-axial extension of rubber: the canonical 1944 data of Treloar (see his book (Treloar 2005)) and a more recent set by Dobrynin and Carrillo (2011). Then we proceed to model each regime of stretch in turn. For the small-to-moderate regime, we show that W must be a function of the two invariants, which rules out the whole class of generalised neo-Hookean materials, for which $W = W(I_1)$ only, including the Yeoh model. We study three representative models (Mooney-Rivlin, Gent-Thomas, Carroll) giving excellent fits in that regime. The conclusion here is that the specific choice of a model is not that important for the small-to-moderate regime, as long as it is not a generalised neo-Hookean material. For the next regime, which corresponds to an upturn in the Mooney plot, we add a strain-hardening term to those models and again the fit is excellent, now across the resulting wider range of data. For the range of extreme stretches, we show how to determine the order of singularity, i.e. how to find out whether the rubber stiffens according to the WLC or the FJC model. Finally we provide models that fit the data over the entire range of experimental data, with errors below 4%. The conclusion is that the term used to capture the asymptotic limiting-chain behavior also captures the earlier strain-hardening regime, and that the number of fitting parameters can be kept to three only, see Figure 1.

In Section 4 we confirm the robustness of our methodical modelling based on simple tension by looking at its predictions for two other types of deformation: simple shear and inhomogeneous rectilinear shear. In this paper we focus on fitting models using uniaxial data only, because it is the most basic problem faced in the applications of the nonlinear theory of elasticity to rubber elasticity, and the most available experimental data. Only once this problem has been tackled and solved can we attack the question of fitting models for rubber using other types of data, for equi-biaxial or multi-axial tension, simple shear, pure shear, inflation, bending, torsion, etc.

Section 5 is a recapitulation of the results and a reflection on their consequences.

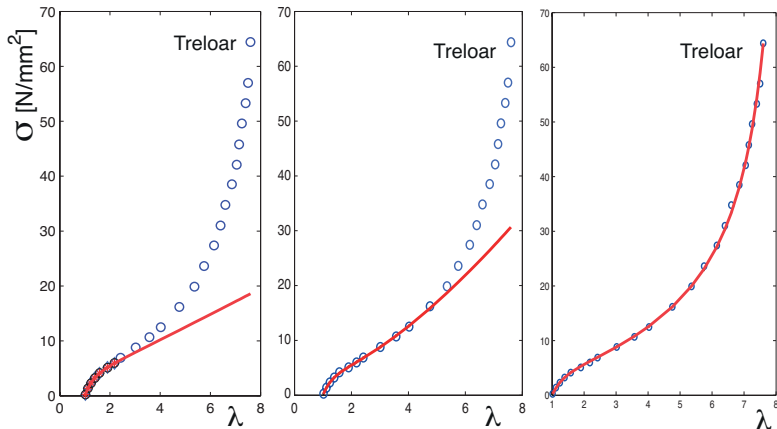


Figure 1: Methodical fitting of the non-linear response of rubber to uniaxial tension (Treloar data). With the Gent-Gent strain energy function, we capture in turn the small-to-moderate strain regime (Section 3.2), the strain hardening regime (Section 3.3), and the limiting-chain regime (Section 3.5).

2 Material modelling

Here we present some basic results of the axiomatic theory of continuum mechanics for hyperelastic materials and determine a consistent measure of the goodness of fit for simple tension data.

2.1 Choice of material parameters

We consider incompressible isotropic materials which are hyperelastic. For these it is possible to define a strain-energy density $W = W(I_1, I_2)$, where $I_1 = \lambda_1^2 + \lambda_2^2 + \lambda_3^2$ and $I_2 = \lambda_1^{-2} + \lambda_2^{-2} + \lambda_3^{-2}$ are the principal invariants of the left Cauchy-Green deformation tensor $\mathbf{B} = \mathbf{F}\mathbf{F}^T$, where \mathbf{F} is the gradient of deformation and the λ_i are the principal stretches of the deformation (the square roots of the eigenvalues of \mathbf{B} .) Another representation of the principal invariants is

$$I_1 = \text{tr}(\mathbf{B}), \quad I_2 = \text{tr}(\mathbf{B}^{-1}). \quad (1)$$

In passing we note that other sets of invariants exist, but that they are equivalent to our choice for all intents and purposes (Saccomandi 2015, Carroll 2011).

This form of the strain-energy density leads to the usual representation formula for the Cauchy stress tensor \mathbf{T} , due to Rivlin (1996)

$$\mathbf{T} = -p\mathbf{I} + 2W_1\mathbf{B} - 2W_2\mathbf{B}^{-1}, \quad (2)$$

where p is the Lagrange multiplier associated with the incompressibility constraint ($\det \mathbf{F} = 1$ at all times) and $W_i = \partial W / \partial I_i$, ($i = 1, 2$).

Materials with strain-energy density functions such that $W = W(I_1)$ only are denoted *generalized neo-Hookean materials*. A prime member of this class is the so-called *neo-Hookean material*

$$W_{\text{nH}}(I_1) = \frac{\mu_0}{2} (I_1 - 3), \quad (3)$$

where the constant $\mu_0 > 0$ is the infinitesimal shear modulus.

Now, establishing which restrictions should be imposed on the strain-energy function to guarantee reasonable physical behavior is known as Truesdell's *Hauptproblem* of the elasticity theory (Truesdell 1956). In this connection we recall the point of view of Ball and James (2002):

At the end of the day, perhaps it would have been realized that Hadamard notions of well-posedness are far too restrictive in the nonlinear setting, that non-uniqueness and even non-existence comprise acceptable behavior, and that there are probably no fundamental restrictions on the strain-energy function at all besides those arising from material symmetry and frame-indifference.

So that we may not expect much from mathematical requirements. We must thus resort to *mechanical arguments*.

First of all, we point out that we dealt with frame-indifference and material symmetry when we chose to write W as a function of the principal invariants (1), see Rivlin (1996). Next, we require as a normalization condition that the strain-energy be zero in the reference configuration: $W(3, 3) = 0$. Also, for incompressible materials, the requirement that the stress is zero in the reference configuration is always satisfied by a suitable choice of the value of p in that configuration.

The next fundamental requirement is linked to the notion of the *generalized shear modulus function* μ , defined as

$$\mu = \mu(I_1, I_2) \equiv 2(W_1 + W_2). \quad (4)$$

In the reference configuration it gives the *infinitesimal shear modulus* μ as

$$\mu_0 = \mu(3, 3). \quad (5)$$

For isotropic incompressible linear materials this is the only significant Lamé modulus and compatibility of the non-linear model with the linear theory requires that $\mu_0 > 0$.

Further, we impose requirements on the class of models incorporating, at the macroscopic level, information about the contour length of the single chain. Hence we require that, as the contour length for the end-to-end distance of the polymeric chain goes to infinity, it is necessary to recover the Gaussian chain model, itself easily connected to the macroscopic neo-Hookean strain energy density (3). Hence, suppose that one of the constitutive parameters contained in the strain-energy density, called J_m (say), is a measure of the model's *limiting-chain extensibility*, the macroscopic analogue of the contour length. For example in the case of a generalised neo-Hookean material, J_m can be an upper bound for $I_1 - 3$ which is an average measure of the squared stretch (Kearsley 1989). In that case we would impose that

$$\lim_{J_m \rightarrow \infty} W = W_{\text{nH}}. \quad (6)$$

A further basic requirement that we may impose on W comes from the *weakly non-linear theory of elasticity*, where the strain energy is expanded in powers of the strain. For instance, by choosing the Green-Lagrange tensor $\mathbf{E} = (\mathbf{F}^T \mathbf{F} - \mathbf{I})/2$ as a measure of strain, the most general fourth-order expansion of incompressible elasticity (Ogden 1974, Hamilton et al. 2004, Destrade and Ogden 2010) can be written in the form

$$W = \mu_0 \text{tr}(\mathbf{E}^2) + \frac{A}{3} \text{tr}(\mathbf{E}^3) + D (\text{tr}(\mathbf{E}^2))^2, \quad (7)$$

where μ_0 is the infinitesimal shear modulus (the only parameter of the linear theory), A is the Landau third-order constant and D is the fourth-order elastic constant. It is now known that in order to capture fully non-linear effects in solids, the fourth-order theory is the *minimal* model to consider. For example, in physical acoustics (Norris 1998), it is necessary to carry out the expansion of W to fourth order to ensure that non-linear effects in shear waves emerge (Hamilton et al. 2004, Destrade et al. 2011); in the elastic bending of blocks made of incompressible soft solids, the onset of non-linearity involves third- as well as fourth-order constants (Destrade et al. 2010); etc. In conclusion we will impose a consistent compatibility with the fourth order weakly non-linear theory, instead of compatibility with linear theory only.

2.2 Fitting to uni-axial data

From now on we concentrate on the data given by the (idealised) homogeneous deformation of *uni-axial extension* resulting from the application of a uni-directional tension. We call λ the stretch in that direction.

It is a simple matter to compute the first and second invariants of the Cauchy-Green deformation tensors, as

$$I_1 = \lambda^2 + 2\lambda^{-1}, \quad I_2 = \lambda^{-2} + 2\lambda, \quad (8)$$

and the *tensile Cauchy stress component* (Ogden 1984) $t = T_{11}$, as $t = \lambda \partial W / \partial \lambda$. In experiments, the current force applied per unit length f_1 is recorded, and by dividing it by the reference cross-sectional area of the sample, we arrive at the *engineering tensile stress* $\sigma = \lambda^{-1} t$. It is given by

$$\sigma(\lambda) = \frac{\partial W}{\partial \lambda} = 2(\lambda - \lambda^{-2}) \left(\frac{\partial W}{\partial I_1} + \lambda^{-1} \frac{\partial W}{\partial I_2} \right). \quad (9)$$

Then, by plotting the $\lambda - \sigma$ curve for $\lambda \geq 1$, we can perform a curve-fitting exercise for a candidate strain energy density W and access the values of its derivatives.

Alternatively, we could plot the $t - \lambda$ curve to access the derivatives of W .

Historically, Rivlin (1996) divided the relationship (9) across by $2(\lambda - \lambda^{-2})$ and plotted the curve obtained by having the resulting left handside as the vertical axis coordinate and λ^{-1} as the horizontal coordinate. This modified version of (9) is the so-called *Mooney Plot*, given by the transform

$$g(z) = \frac{\partial W}{\partial I_1} + z \frac{\partial W}{\partial I_2}, \quad \text{where} \quad g(z) := \frac{\sigma(\lambda)}{2(\lambda - \lambda^{-2})}, \quad z := \lambda^{-1}. \quad (10)$$

In this approach we plot the $z - g$ curve for the range $0 < z \leq 1$ to access the values of the derivatives of W . The practical effect of the Mooney transform is to map the range $1 \leq \lambda \leq 2$ (where the measurements are the most reliable) over 50% of the z -domain.

Now, let us consider the experimental data of stretches and engineering stresses (λ_i, σ_i) for $i = 1, \dots, m$ in the *engineering space* \mathcal{E} , of stretches and Cauchy stresses (λ_i, t_i) for $i = 1, \dots, m$ in the *Cauchy space* \mathcal{C} , and the corresponding data in the *Mooney space* \mathcal{M} , obtained by the Mooney transform: $(z_i, g_i) := (\lambda_i^{-1}, \sigma_i / [2(\lambda_i - \lambda_i^{-2})])$ for $i = 1, \dots, m$, where m is the number of measurements in the uni-axial test.

At this juncture we emphasize that different fitting procedures are possible and that the choice of a given procedure may have an impact on our modeling considerations.

2.3 Goodness of fit

In general, let $\mathbf{p} = [p_1, \dots, p_n]$ be the set of material parameters involved in the definition of the strain energy W , that have to be identified by *matching*,

as best as we can, the data with the desired mathematical model for W . For example, for the neo-Hookean solid (3) we have $\mathbf{p} = [\mu_0]$ and for the fourth-order elasticity model (7) we have $\mathbf{p} = [\mu_0, A, D]$. To evaluate the best-fit parameters \mathbf{p} we solve a Least Squares (LS) problem, which can be linear or non-linear depending on the functional dependence of the strain energy densities W from \mathbf{p} .

To quantify the goodness of fit, we define on the one hand the following (*absolute*) *residuals* in the spaces \mathcal{E} , \mathcal{C} , and \mathcal{M} ,

$$\sigma(\lambda_i; \mathbf{p}) - \sigma_i, \quad t(\lambda_i; \mathbf{p}) - t_i, \quad g(z_i; \mathbf{p}) - g_i, \quad (11)$$

($i = 1, \dots, m$), respectively, and on the other hand, the following *relative residuals*,

$$r_i^R(\mathbf{p}) = \frac{\sigma(\lambda_i; \mathbf{p})}{\sigma_i} - 1 = \frac{t(\lambda_i; \mathbf{p})}{t_i} - 1 = \frac{g(z_i; \mathbf{p})}{g_i} - 1, \quad (12)$$

($i = 1, \dots, m$) The latter equalities, due to the Equations (9)-(10), show that the *relative residuals are the same in the Engineering, Cauchy and Mooney spaces*. Moreover, (12) shows that the *relative errors* are non-dimensional quantities and can be expressed in percentage, as opposed to the absolute residuals.

Then in the classical LS setting, the strategy is to minimize either of the following Euclidean norms by varying \mathbf{p} ,

$$\sum_{i=1}^m [\sigma(\lambda_i; \mathbf{p}) - \sigma_i]^2, \quad \sum_{i=1}^m [t(\lambda_i; \mathbf{p}) - t_i]^2, \quad \sum_{i=1}^m [g(z_i; \mathbf{p}) - g_i]^2. \quad (13)$$

In this paper we make the choice of *minimising the relative errors* in the two norm, that is

$$\|\mathbf{r}_R(\mathbf{p})\|_2^2 = \sum_{i=1}^m r_i^R(\mathbf{p})^2, \quad (14)$$

because it best captures our attempts at optimising the global curve fitting exercise over a large range of stretches. It is worth noting that this approach corresponds to a classical weighted LS procedure in the Engineering, Cauchy and Mooney spaces, where the weights are $w_i = 1/\sigma_i^2$, $w_i = 1/t_i^2$, $w_i = 1/g_i^2$, respectively.

We shall leave aside minimisation of classical absolute residuals from now on because we found that it gives large relative errors in the small-to-moderate range of extension, which is not desirable from experimental and modelling points of view. Moreover, the best-fit parameters obtained by

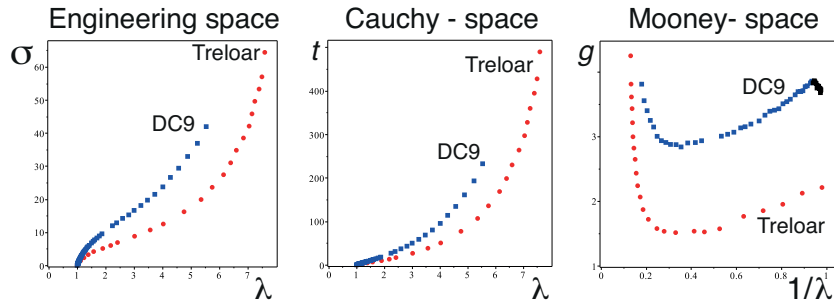


Figure 2: Blue squares: DC9 data; red circles: Treloar’s data. Left (middle) plot: the tensile engineering (Cauchy) stress σ (t) in N/mm^2 against the stretch λ . Right plot: the corresponding $g - z$ Mooney plots. Three regimes are clearly identified in the \mathcal{M} -space as we stretch the samples (decreasing $z = 1/\lambda$). Linear decrease: *small-to-moderate regime*; upturn: *strain hardening regime*; rapid stiffening: *limiting-chain effect regime*. The first 14 points of the DC9 Mooney plot are greyed out as we must ignore their contribution (see main text).

minimising absolute residuals are not the same when we use the engineering stress data, the Cauchy stress data, or the Mooney plot data, which is a problem as the parameters in a strain energy density should be independent of the choice of stress measure.

To quantify the goodness of our fits, we will record the maximal relative error $\text{err}^* = \|\mathbf{r}_{\mathbf{R}}(\mathbf{p}^*)\|_{\infty}$ over the range of interest, defined as follows

$$\text{err}^* = \max_i \left| \frac{\sigma(\lambda_i; \mathbf{p}^*)}{\sigma_i} - 1 \right| = \max_i \left| \frac{t(\lambda_i; \mathbf{p}^*)}{t_i} - 1 \right| = \max_i \left| \frac{g(z_i; \mathbf{p}^*)}{g_i} - 1 \right|. \quad (15)$$

3 Numerical Results

3.1 Experimental data

To test our models, we will consider two comprehensive sets of data recorded for the uni-axial extension of rubber samples. The first set is due to Treloar (2005), dating back to his canonical 1944 experiments. For that set we use the original tabulated data, with the engineering stress measured in N/mm^2 units, see raw data consisting of 24 points below. The second set is due to Becker and Kruger (1972), as collected by Dobrynin and Carrillo (2011): we will use the data collected in their set labelled ‘DC9’; it consists of 48 data

points.

$$\begin{aligned}\lambda &= [1.02, 1.12, 1.24, 1.39, 1.58, 1.90, 2.18, 2.42, 3.02, 3.57, 4.03, 4.76, \\ &\quad 5.36, 5.75, 6.15, 6.4, 6.6, 6.85, 7.05, 7.15, 7.25, 7.40, 7.5, 7.6], \\ \sigma &= [0.26, 1.37, 2.3, 3.23, 4.16, 5.10, 6.0, 6.9, 8.8, 10.7, 12.5, 16.2, 19.9, \\ &\quad 23.6, 27.4, 31, 34.8, 38.5, 42.1, 45.8, 49.6, 53.3, 57, 64.4].\end{aligned}\quad (16)$$

Plotting the data in the Mooney space \mathcal{M} clearly delineates *three regimes of extension* for the elastomers, see Figure 2. Starting from $z = \lambda^{-1}$ at value 1 (no extension) and decreasing (extension), we see at first a linear decrease of g with z for *small-to-moderate deformations*. Then, around a value for z of 0.3 (stretch of 230% or so), an *upturn* occurs as g goes through a minimum. Finally we enter the *large deformation regime*, where the reduced tensile stress rises sharply and considerably.

Before we move on to model each regime in turn, we note that we had to exclude the first 14 points from the original DC9 data (greyed in the Mooney plot of Figure 2), because they prevented the DC9 Mooney plot from having a linear decrease in the small-to-moderate regime. For reasons explained later, every soft solid *must* have such a linear decrease. The reason for the experimental discrepancy presented by the first 14 points is not known, but is probably due to non-optimal accuracy regime for the load-cell in the low load regime and/or the presence of a slight slack of the sample in its starting position.

3.2 From small to moderate strains

In this section, we focus on the term in the strain energy that will model the small-to-moderate regime of deformation for the samples. We identify this region by the *linear part* of the Mooney plot occurring before the upturn, see Figure 2. Hence we perform the curve-fitting exercise on the first N_0 data points only, where we determine N_0 by conducting a model-dependent sensitivity analysis (to be detailed later).

First we see that the neo-Hookean model (3) is incapable of reproducing the simple extension data in any meaningful way. That is because, for W_{NH} , the Mooney plot formula (10) yields

$$g(z) = \mu_0/2, \quad (17)$$

giving thus an horizontal line in the \mathcal{M} -space. The top three panels of Figure 3 illustrate well the resulting unphysical character of the predicted behaviour. The corresponding relative errors are thus predictably large.

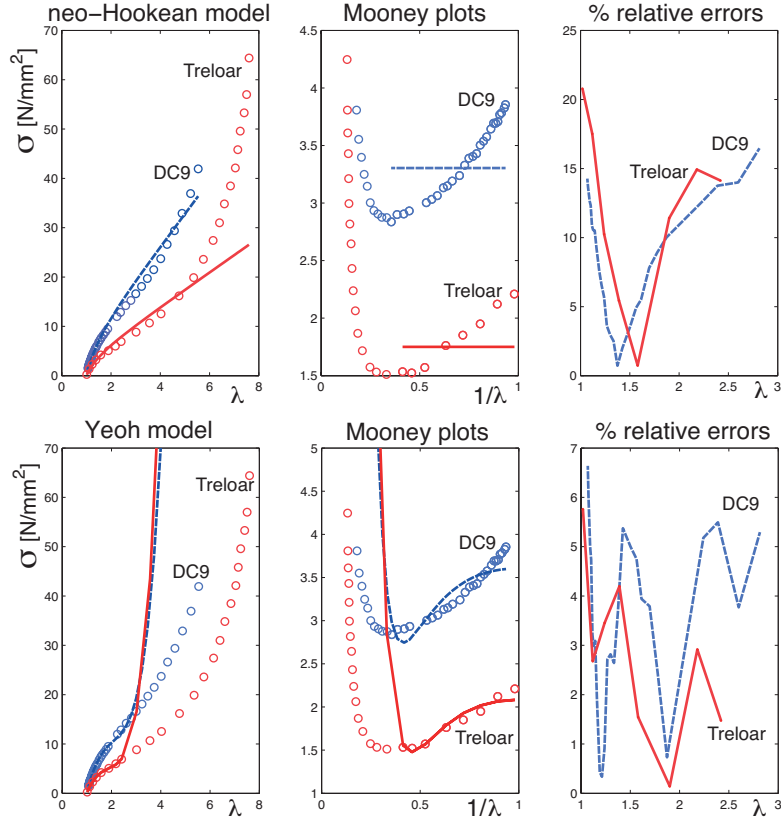


Figure 3: Least-Square fitting of the *neo-Hookean model* (top row) and the *Yeoh model* (bottom row) in the small-to-moderate regime. For Treloar’s data, the best-fit curve is the red full curve and for the DC9 data, the best-fit curve is the blue dashed curve. Left panels: fitting results in the engineering space on the first N_0 data points; Center panels: the corresponding Mooney plots; Right panels: corresponding % relative errors.

For a polynomial dependence of W on I_1 , we can consider the Yeoh strain energy density (Yeoh 1990)

$$W_{\text{Yeoh}} = c_1(I_1 - 3) + c_2(I_1 - 3)^2 + c_3(I_1 - 3)^3, \quad (18)$$

where the c_i are constitutive parameters (by (5), the infinitesimal shear modulus of this material is $\mu = 2c_1$). This model gives of course a better fit in the small-to-moderate region than the neo-Hookean potential, see Figure 3, lower panels, and Table 1.

However, as is evident from the formula (10), we must include a dependence on the second principal invariant I_2 in order to make meaningful progress.

material:	neo-Hookean		Yeoh			
	μ_0	err*	c_1	c_2	c_3	err*
Treloar	3.7235	18.50%	2.1317	-0.3624	0.3624	3.98%
DC9	6.6087	16.47%	3.6048	-0.2339	0.0212	6.64%

Table 1: Material parameters for the neo-Hookean and the Yeoh models, obtained by linear curve fitting of Treloar’s and DC9 data over the small-to-moderate range (first $N_0 = 7$ data points for the former and first $N_0 = 25$ points for the latter). The maximal relative error err* over the first N_0 points is also displayed. The corresponding curves and relative errors are shown in Figure 3.

Hence we will consider in turn the following two classical strain energies: the *Mooney-Rivlin model* (Mooney 1940),

$$W_{\text{MR}} = \frac{1}{2}C_1(I_1 - 3) + \frac{1}{2}C_2(I_2 - 3), \quad (19)$$

and the *Gent-Thomas model* (Gent and Thomas 1958),

$$W_{\text{GT}} = \frac{1}{2}C_1(I_1 - 3) + \frac{3}{2}C_2 \ln\left(\frac{I_2}{3}\right); \quad (20)$$

and also the more recent *Carroll model* (Carroll 2011)

$$W_{\text{C}} = \frac{1}{2}C_1(I_1 - 3) + \sqrt{3}C_2(\sqrt{I_2} - \sqrt{3}). \quad (21)$$

These are two-parameter models, where C_1 and C_2 are the material constants to be found from the best-fit procedure. As noted by Carroll (2011), all three belong to the class of strain energies proposed by Klingbeil and Shield (1964). When these strain energies are expanded up to third order in the powers of the Green-Lagrange strain tensor \mathbf{E} , we find that they all give

$$W = (C_1 + C_2) \text{tr}(\mathbf{E}^2) - \frac{4}{3}(C_1 + 2C_2) \text{tr}(\mathbf{E}^3), \quad (22)$$

giving the following direct correspondence with the weakly non-linear elasticity expansion (7), when stopped at the same order (Ogden 1974, Destrade et al. 2010, Destrade and Ogden 2010)

$$\mu_0 = C_1 + C_2, \quad A = -4(C_1 + 2C_2). \quad (23)$$

To determine rigorously how many data points we should take for the small-to-moderate region, we performed a sensitivity analysis for all three models. We found that the maximal relative error is at its lowest value when

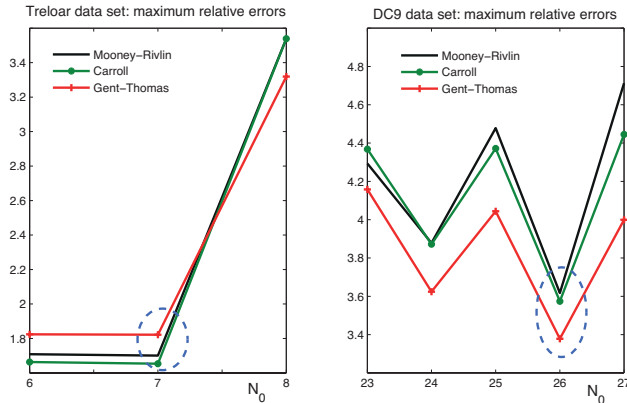


Figure 4: Sensitivity analysis to determine the extent of the “small-to-moderate” range. Here the models are fitted in the range $2 \leq \lambda \leq 3$ and the maximum relative error is recorded in terms of the number of data points considered.

$N_0 = 7$ for the Treloar data set and $N_0 = 26$ for the DC9 data set, see Figure 4.

We see from the resulting best-fit curves of Figure 5 that, as expected, the I_2 -dependence is precisely the missing ingredient to obtain excellent agreement in the small-to-moderate regime. The figure is eloquent on two features.

First, the relative errors are dramatically reduced over that regime, to less than 1.8% for Treloar’s data and less than 3.6% for the DC9 data, see Table 2. This improvement is achieved with a set of only two material parameters $\mathbf{p} = [C_1, C_2]$ at our disposal, in contrast to the Yeoh model (18) which gave much higher errors with a set of three fitting parameters $\mathbf{p} = [c_1, c_2, c_3]$.

Second (as noted earlier by Carroll (2011)), the actual dependence of W on I_2 does not matter much, with all three models (19), (20), (21) performing equally well. This is not altogether surprising in view of the third-order expansion (22) and its universality and relevance to the small-to-moderate range of extension. In effect, the equivalence of the Mooney-Rivlin strain energy and the third-order expansion shows that every incompressible isotropic hyperelastic solid must present a linear decrease at first in the Mooney space.

In the next section we denote the functional dependence of W on I_2 generically by $f(I_2)$ to save space.

3.3 Strain-hardening regime

We now move on to the *strain-hardening regime*, which is how we called the range of data corresponding to the *upturn* in the Mooney plots, see Figure

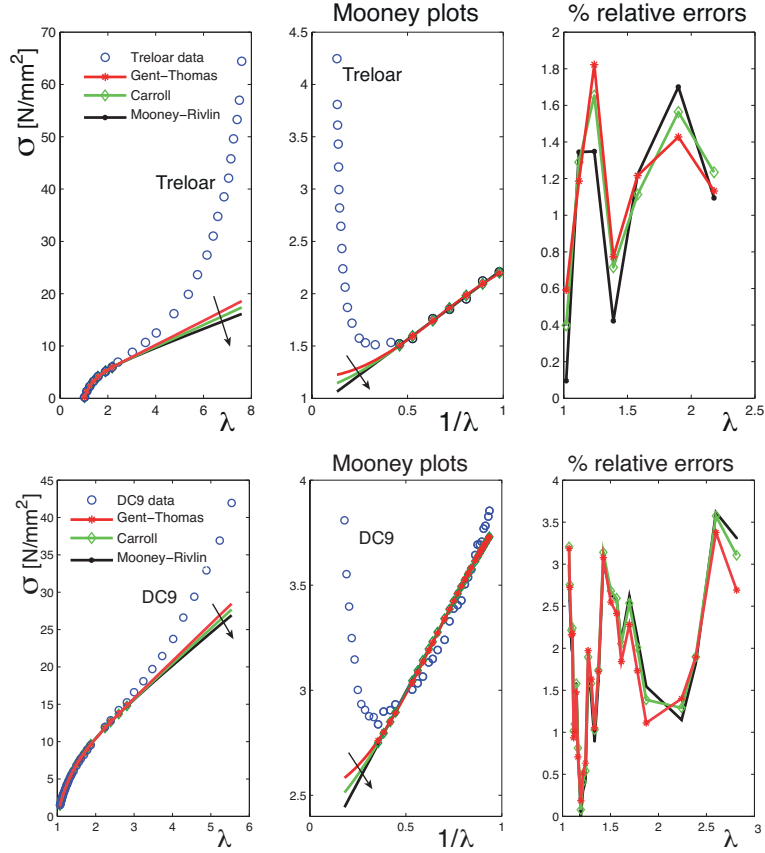


Figure 5: Least-square fitting in the small-to-moderate regime: result of the fitting with I_2 corrections by Mooney-Rivlin, Carroll and Gent-Thomas models. The differences in best-fitting performance between the models are negligible. Top row: Fitting to Treloar's data; Bottom row: Fitting to DC9 data. When the plots are hard to distinguish one from another, an arrow shows the order Gent-Thomas/Carroll/Mooney-Rivlin.

2. Thus, here we will perform our curve fitting exercises on the $N_0 + N_p$ first data points, where N_p is the number of points required to capture that the Mooney plot has gone through a minimum. For our two sets of data here, we take $N_p = 5$.

Keeping in line with our methodical approach to modeling we now add a power-law term to the strain energy density of the previous section and consider W in the form

$$W = \frac{1}{2}C_1(I_1 - 3) + C_2f(I_2) + C_3\frac{3^{1-n}}{2n}(I_1^n - 3^n), \quad (24)$$

where $C_3 > 0$ (N/mm²) and $n > 0$ (non-dimensional) are constants (Lopez-

	C_1	C_2	err*	μ_0	A
material:	Mooney-Rivlin				
Treloar	1.7725	2.7042	1.70%	4.4767	-28.724
DC9	4.2671	3.4329	3.62%	7.7000	-44.532
material:	Gent-Thomas				
Treloar	2.3992	2.0348	1.82%	4.4340	-25.875
DC9	5.0400	2.6016	3.38%	7.6416	-40.973
material:	Carroll				
Treloar	2.1580	2.2891	1.65%	4.4471	-26.945
DC9	4.7544	2.9006	3.57%	7.6550	-42.222

Table 2: Material parameters C_1 and C_2 (N/mm²) for the Mooney-Rivlin, Gent-Thomas and Carroll models, obtained by linear curve fitting of Treloar’s and DC9 data over the small-to-moderate range (first $N_0 = 7$ data points for the former and first $N_0 = 26$ points for the latter). The maximal relative error err* over the first N_0 points is also displayed, as well as μ_0 and A (N/mm²), the corresponding constants of second and third order elasticity, respectively. The corresponding curves and relative errors are shown in Figure 5.

Pamies 2010). As noted by Carroll (2011), as the tensile stretch λ increases, the principal force associated with an energy term I_1^n behaves as λ^{2n-1} (Note that we could have chosen to add a I_2^m term instead, in which case the force would behave as λ^{4m-1} .) Hence, for an ideal (no solvent) polymer, $n = 1$ and we recover the Gaussian Chain model; for a polymer in a good solvent, $n = 5/4$ and we recover the Pincus correction of the force behaving as $\lambda^{3/2}$.

Here we wish to model the strain-stiffening as illustrated by the upturn in the Mooney plot. As λ increases, I_1^n behaves as λ^{2n} and σ as $\lambda^{2(n-1)}$. Hence in the Mooney plot, as z goes towards zero, $g(z)$ behaves as $z^{-2(n-1)}$, indicating that $n > 1$ is required for an upturn.

We point out that the optimisation of the material parameter set $\mathbf{p} = [C_1, C_2, C_3, n]$ is a *non-linear* procedure. In general, non-linear curve fitting exercises lead to some serious computational problems, the most common being the emergence of multiple minima for the same level of error, see the discussion by Ogden et al. (2004) for rubber models. Also, the choice of an adequate initial guess is a crucial issue in order to avoid false minima (Motulsky and Christopoulos 2004). To circumvent these problems we propose the following ad hoc procedure.

For definiteness we consider that the optimal value of n should be found in the range $1.0 < n < 2.5$: the lower bound indicates a departure from

the linear fit of the small-to-moderate Mooney plot region and, at twice the Pincus value, the upper bound is a reasonable ceiling to capture the upturn of the Mooney plot prior to the large strain stiffening regime.

We limit the range of data to the $N_0 + N_p$ first points, spanning the small-to-moderate regime (linear variation in the Mooney plot) and the strain-hardening regime (upturn in the Mooney plot). Then we fix n at the beginning of the $1 < n < 2.5$ range, at $n = 1.01$ say, and perform the fit for the reduced set $\mathbf{p} = [C_1, C_2, C_3]$. This fit is *linear* and thus removes the risk of multiple minima and the requirement of a good initial guess. Then we increase n to span the range and record the corresponding maximum relative errors $\text{err}(n)$. Finally we keep the optimal value of n , corresponding to $\text{err}^* = \min_{1 < n < 2.5} \text{err}(n)$.

For Treloar's data we fix $N_0 + N_p = 7 + 5$, and for the DC9 data we take $N_0 + N_p = 24 + 5$. For the fitting of the former set, the Gent-Thomas model with a strain-hardening correction gives the lowest error, while for the later set it is the Mooney-Rivlin model with a strain-hardening correction which performs best. However, similarly to the previous section, the differences in performance between the three models are negligible, see Table 3 for a summary. Overall the fit is excellent over the small-to-moderate and strain-hardening regimes, as attested by the low values of the relative errors, around or less than 2%.

In Table 3 we also report the corresponding constants of weakly non-linear elasticity μ_0 , A , and D . They are obtained by expanding W in (24) up to fourth order in the Green-Lagrange strain tensor. We find that now

$$\mu_0 = C_1 + C_2 + C_3, \quad A = -4(C_1 + 2C_2 + C_3), \quad (25)$$

while for the fourth-order elastic constant D in (7) we have

$$D = C_1 + 3C_2 + \frac{1}{3}C_3(n+2), \quad C_1 + \frac{8}{3}C_2 + \frac{1}{3}C_3(n+2), \quad C_1 + \frac{17}{6}C_2 + \frac{1}{3}C_3(n+2), \quad (26)$$

for the Mooney-Rivlin, Gent-Thomas, and Carroll models with a strain-hardening term, respectively. We notice that there is no strong continuity for the C_1 and C_2 parameters from Table 2 to Table 3, reflecting that these parameters are simply the result of a curve fitting exercise. The weakly non-linear elasticity constants μ_0 and A however carry consistently from one model to the other.

In this section we showed that a strain energy with three terms and four material parameters can cover the range of 500% extension for Treloar's data ($1 \leq \lambda \leq 6$) and 300% extension for the DC9 data ($1 \leq \lambda \leq 4$). It is worth noting that for each model the solution for the optimal set of parameters is unique and the problems are not ill-conditioned.

	C_1	C_2	C_3	n	err*	μ_0	A	D
material	Mooney-Rivlin + strain-hardening							
Treloar	1.7716	2.6135	0.02725	1.6652	2.05%	4.412	-28.10	10.83
DC9	3.6974	3.9934	0.0542	1.0939	1.21%	7.746	-46.96	16.71
material	Gent-Thomas + strain-hardening							
Treloar	2.0489	1.8781	0.8911	1.6798	1.78%	4.818	-26.78	8.284
DC9	4.6837	2.9426	0.0434	1.0500	1.63%	7.670	-42.45	13.55
material	Carroll + strain-hardening							
Treloar	2.1541	2.2080	0.02495	1.6066	1.88%	4.387	-26.38	9.612
DC9	4.3052	3.3351	0.0495	1.0500	1.48%	7.6898	-44.10	14.77

Table 3: Material parameters C_1 , C_2 , C_3 (N/mm²) and n for the Mooney-Rivlin, Gent-Thomas and Carroll models augmented with a power-law term, obtained by curve fitting of Treloar’s and DC9 data over the small-to-moderate range and the strain-hardening regime (first $N_0 + N_p = 7 + 5$ data points for the former and first $N_0 + N_p = 24 + 5$ points for the latter). The smallest relative error err* over the first $N_0 + N_p$ points is also displayed, as well as the elastic constants of fourth-order weakly nonlinear elasticity μ_0 , A and D . The corresponding curves and relative errors are shown in Fig. 6.

If we wish to go further and also capture the behaviour of soft matter in a regime of extreme extension ($6 \leq \lambda \leq 8$ and $4 \leq \lambda \leq 6$, respectively), we have to recognise that the corresponding stiffening of the curve is associated with a singularity of the fitting function. In other words, *limiting-chain effects* come to dominate in the latter regime and impose an asymptotic barrier. In the next section we present a method to determine the order of the singularity by examination of the experimental data.

3.4 Estimate of the order of singularity: FJC vs WLC

In this section and the next, we focus on the *extreme stretch range*, where the material stiffens rapidly with strain. First we consider only the last N_f points of the force-extension data, and estimate how fast the data curve “blows up”.

Assume that in the large stretch range, the tensile force behaves as

$$f = \sigma A_0 \sim \frac{c}{(1 - \lambda/\lambda_m)^k}, \quad (27)$$

where A_0 is the cross-section area of the sample in the undeformed state, c is a constant, $\lambda = \lambda_m$ indicates the location of the unknown vertical asymptote,

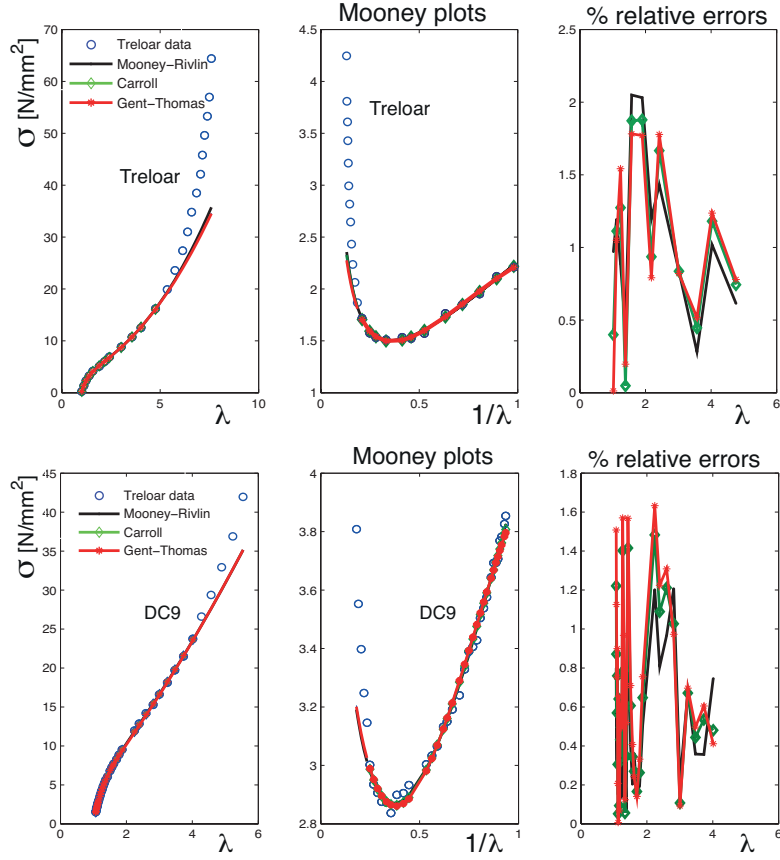


Figure 6: Least-square fitting in the small-to-moderate and the strain-hardening regimes: Mooney-Rivlin, Carroll and Gent-Thomas models with power-law correction when the first $N_0 + N_1$ data points are considered. Top row: Fitting to Treloar’s data (first 7+5 data points); Bottom row: Fitting to DC9 data (first 26+5 points). The ‘best’ fitting results are obtained by the Gent-Thomas model and by the Mooney-Rivlin model, respectively, although the differences with the other models are minute and the plots are undistinguishable.

and k is the *order of singularity*: $k = 1$ for the FJC model and $k = 2$ for the WLC model.

In logarithmic coordinates we have

$$\log(\sigma) = \log(c/A_0) - k \log(1 - \lambda/\lambda_m), \quad (28)$$

suggesting a linear regression procedure to identify k , as follows. For the last N_f data points, we can calculate $\log(\sigma)$. We also know that λ_m is greater than λ_f , the largest stretch reported in the experiments (hence $\lambda_f = 7.6$ for the Treloar set, see (16), and $\lambda_f = 5.54$ for the DC9 set). Then we start

by fixing $\lambda_m = \lambda_f + 0.001$, say, and plot $\log(\sigma)$ against $\log(1 - \lambda/\lambda_m)$ to perform a linear fit. We estimate the corresponding maximal relative error and repeat the procedure for a higher value of λ_m , and so on.

Here for both data sets, we find that the maximal relative error goes through a minimum as λ_m increases. When it is at its minimal value, we can say that we have identified the actual order of singularity k^* and the actual limiting stretch λ_m^* .

In Figure 7, we report these results for the Treloar's and DC9 data, in the upper and lower panels, respectively, where the optimal solutions yielding k^* and λ_m^* are highlighted in red. For Treloar's data, we take $N_f = 9$, and find $\lambda_m^* = 8.72$ and $k^* = 0.962$, with a maximal relative error of 2.1%, indicating a *first order singularity* location for large deformations. For the DC9 rubber data set, we take $N_f = 5$ and find $\lambda_m^* = 10.6$, $k^* = 2.03$ with a maximal relative error of 0.6%, clearly pointing out to a *second-order singularity*.

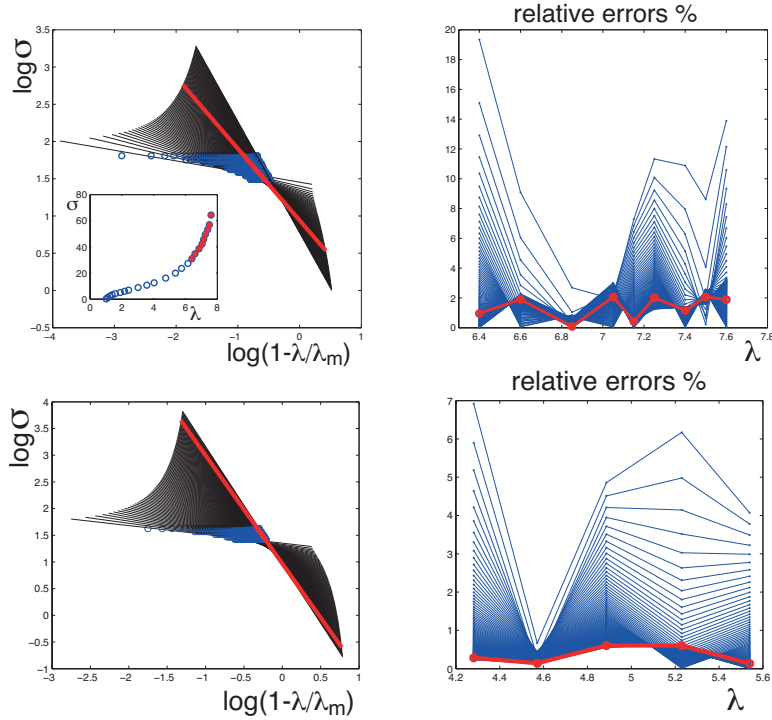


Figure 7: Estimating the order of singularity k and the maximal stretch of the chain limit λ_m , using the last 9 points for Treloar's data (top) and the last 5 points for the DC9 data (bottom). Left subplots report the linear fittings, right subplots report the corresponding relative errors. The optimal solutions yielding k^* and λ_m^* are highlighted by the thick red lines.

If our goal is to provide a 1-dimensional interpretation of the data at extreme stretches, then our method shows that the rubber studied by Treloar behaves according to the FJC model, while the DC9 rubber behaves according to the WLC model.

The FJC model is easily extended to a 3-dimensional strain energy function, as is often captured by the Arruda and Boyce (1993) 8-chain model, itself represented well by the phenomenological Gent model (Gent 1996),

$$W = -\frac{1}{2}C_1J_m \ln \left(1 - \frac{I_1 - 3}{J_m} \right). \quad (29)$$

Here $C_1 > 0$ is the initial shear modulus and $J_m > 0$ is a stiffening (limiting-chain) parameter.

The WLC model is not easily translated into a 3-dimensional strain energy function, see Ogden et al. (2006). Dobrynin and Carrillo (2011) proposed to mimic the WLC behavior with the following phenomenological model

$$W = G \left[\frac{I_1}{6} + \beta^{-1} \left(1 - \beta \frac{I_1}{3} \right)^{-1} \right], \quad (30)$$

where $G > 0$ and is the “network infinitesimal shear modulus” and β is a stiffening parameter. In passing, note that by (5) the infinitesimal shear modulus is $G(\frac{1}{2} + \frac{1}{\beta(\beta-1)})$. Note also that this model (30) is a special case of the family of models presented by Horgan and Saccomandi (2003)

Guided by these models, the next section will try to capture the non-linear behavior of the Treloar data and its first-order singularity by invoking the first model above, and the behavior of the DC9 data and its second-order singularity with the second model above.

3.5 Limiting-chain effect

In this section, we bring together all our accumulated knowledge to reproduce the non-linear behaviour of the rubber tested by Treloar over the *entire range of experimental stretches*.

The natural summation of our analysis so far is that the whole model to be studied should be given, for the Treloar data, by following form

$$W = -\frac{1}{2}C_1J_m \ln \left(1 - \frac{I_1 - 3}{J_m} \right) + C_2f(I_2), \quad (31)$$

and for the DC9 data, by

$$W = \frac{(1 - \beta^2)}{2(3 - 2\beta + \beta^2)} C_1 \left[I_1 - 3 + 6\beta^{-1} \left(1 - \beta \frac{I_1}{3} \right)^{-1} - 6\beta^{-1} (1 - \beta)^{-1} \right] + C_2 f(I_2). \quad (32)$$

(Note that we added constant terms to this latter expression in order to insure that $W(3, 3) = 0$.)

Here the main difficulty is to identify the optimal value of the limiting-chain parameters J_m or β , because their presence implies that the fitting procedure is a *non-linear* least-square optimization problem. A possible consequence is that a set $\mathbf{p} = [C_1, C_2, J_m]$ or $[C_1, C_2, \beta]$ could be wrongly identified as the optimal one, while there exist other minima giving a better or similar error (Ogden et al. 2004, Motulsky and Christopoulos 2004).

To investigate fully the nature of our optimal set, first we solved the non-linear least squares (NLS) problem by applying the `Lsqcurvefit` routine in Matlab and the `NonlinearFit` routine in Maple, both based on the Levenberg-Marquardt method. Second, since the models contain only one non-linear term, we were also able to apply the VARPRO method devised by Golub and Pereyra (2003). This ‘Variable Projection method’ algorithm is designed for non-linear LS problems where some of the parameters to be identified appear in linear terms, as here. We used a recent Matlab routine (O’Leary and Rust 2013), updated and improved with respect to the original Fortran routine. Third, we used a ‘semi-linear’ approach. In that case we identified the values of the constants C_1, C_2 by a linear fit on the first $N_0 + N_1$ data points. Then we varied the value of the stiffening parameter J_m or β and recorded the corresponding maximum relative error. Then we kept the value of J_m or β giving the lowest relative error over the range.

In the end, these three strategies yielded very similar results, with small differences in the values of the constants and with low error, comparable with the experimental error that can be expected from uni-axial tension experiments. There is little value in presenting all the results of all three procedures and instead we just present those of the NLS routines, which are the simplest to implement.

For completeness and comparison, we used both models above on both the Treloar and the DC9 data. We called them GMR, GG, GC and DCMR, DCG, DCC, corresponding to the Gent (31) or Dobrynin and Carrillo (32) models, respectively, with an I_2 dependence of the Mooney-Rivlin, Gent, and Carroll type, in turn. Notice that the GG model first appeared in (Pucci and Saccomandi 2002) and the DCMR model in (Dobrynin and Carrillo 2011).

We also calculated the corresponding constants of second- and third- order elasticity, as

$$\mu_0 = C_1 + C_2, \quad A = -4(C_1 + 2C_2), \quad (33)$$

for all models, while the constant of fourth-order elasticity is

$$D = \frac{J_m+1}{J_m}C_1 + 3C_2, \quad \frac{J_m+1}{J_m}C_1 + \frac{8}{3}C_2, \quad \frac{J_m+1}{J_m}C_1 + \frac{17}{6}C_2, \quad (34)$$

for the GMR, GG, and GC models, respectively, and

$$D = \frac{13-15\beta+9\beta^2-3\beta^3}{3(1-\beta)(3-2\beta+\beta^2)}C_1 + 3C_2, \quad \frac{13-15\beta+9\beta^2-3\beta^3}{3(1-\beta)(3-2\beta+\beta^2)}C_1 + \frac{8}{3}C_2, \quad \frac{13-15\beta+9\beta^2-3\beta^3}{3(1-\beta)(3-2\beta+\beta^2)}C_1 + \frac{17}{6}C_2, \quad (35)$$

for the DCMR, DCG, and DCC models, respectively.

In Table 4 we collected the results of the curve fitting exercises over the whole range of available data for the Treloar data, and similarly in Table 5 for the DC9 data.

	C_1	C_2	J_m	err*	μ_0	A	D
GMR	2.1531	2.1304	74.74	5.76%	4.283	-25.66	8.573
GG	2.4401	1.9511	78.33	3.38%	4.391	-25.37	7.674
GC	2.3319	2.0077	76.82	4.70%	4.340	-25.39	8.051
	C_1	C_2	β	err*	μ_0	A	D
DCMR	1.9542	2.2548	0.02966	5.32%	4.209	-25.85	9.631
DCG	2.2716	2.0134	0.02787	4.87%	4.285	-25.19	8.699
DCC	2.1524	2.9426	0.02858	4.24%	4.245	-25.35	8.736

Table 4: Material parameters C_1 , C_2 (N/mm²) and J_m or β for the Gent (top) or Dobrynin-Carrillo (bottom) version of the Mooney-Rivlin, Gent-Thomas and Carroll models, obtained by curve fitting of Treloar's data over the entire range of available data. The smallest relative error err* is also displayed, as well as the elastic constants of fourth-order weakly nonlinear elasticity μ_0 , A and D .

For all models, the fit is excellent. Hence with *only three parameters*, we are able to cover the full reported data with an error that compares favourably with the experimental error (recall that Treloar reported values with only three significant digits, see (16)). In particular, the 'Gent-Gent model' (Ogden et al. 2004, Pucci and Saccomandi 2002)

$$W = -\frac{1}{2}C_1J_m \ln \left(1 - \frac{I_1 - 3}{J_m} \right) + \frac{3}{2}C_2 \ln \left(\frac{I_2}{3} \right), \quad (36)$$

	C_1	C_2	J_m	err*	μ_0	A	D
GMR	3.9770	3.7662	64.16	2.70%	7.743	-46.04	15.34
GG	4.7472	2.9650	76.48	2.59%	7.712	-42.71	12.72
GC	4.4597	3.2536	70.73	2.74%	7.713	-43.87	13.74
	C_1	C_2	β	err*	μ_0	A	D
DCMR	3.8024	3.7673	0.0327	2.69%	7.492	-45.04	16.77
DCG	4.5773	2.9582	0.0275	2.60%	7.456	-41.66	14.48
DCC	4.2062	3.2487	0.0297	2.75%	7.455	-42.81	14.83

Table 5: Material parameters C_1 , C_2 (N/mm²) and J_m or β for the Gent (top) or Dobrynin-Carrillo (bottom) version of the Mooney-Rivlin, Gent-Thomas and Carroll models, obtained by curve fitting of the DC9 data over the entire range of available data.

gives a maximal relative error of less than 3.4% for the Treloar data and less than 2.6% for the DC9 data, see plots in Figure 8.

In fact we find that the GG model can be used also to capture the small-to-moderate and strain-hardening regimes only (first $N_0 + N_p$ data points), so that the model (24) with a power-law term can be advantageously replaced with the Gent-Gent model, see Figure 1.

4 Simple and rectilinear shear

Now it remains to figure out how robust and predictive our results are with respect to other deformations. For instance, Ogden et al. (2004) showed that two different Ogden models could give the same excellent fit for uniaxial tension and widely different predictions for rectilinear shear, thereby invalidating them.

Here we first consider the *simple shear deformation*,

$$x = X + KY, \quad y = Y, \quad z = Z, \quad (37)$$

where the constant K is the amount of shear. This deformation is used to idealise some experimental test protocols such as the *double sandwich test* and the *quadruple shear test* (Brown 2006). However, it is not easy to find simple shear test data in the literature on non-linear elastic solids, for the reasons discussed by Destrade et al. (2012): in non-linear elasticity theory, simple shear is not due to a pure shear stress field, and normal stress differences have to be taken into account and controlled.

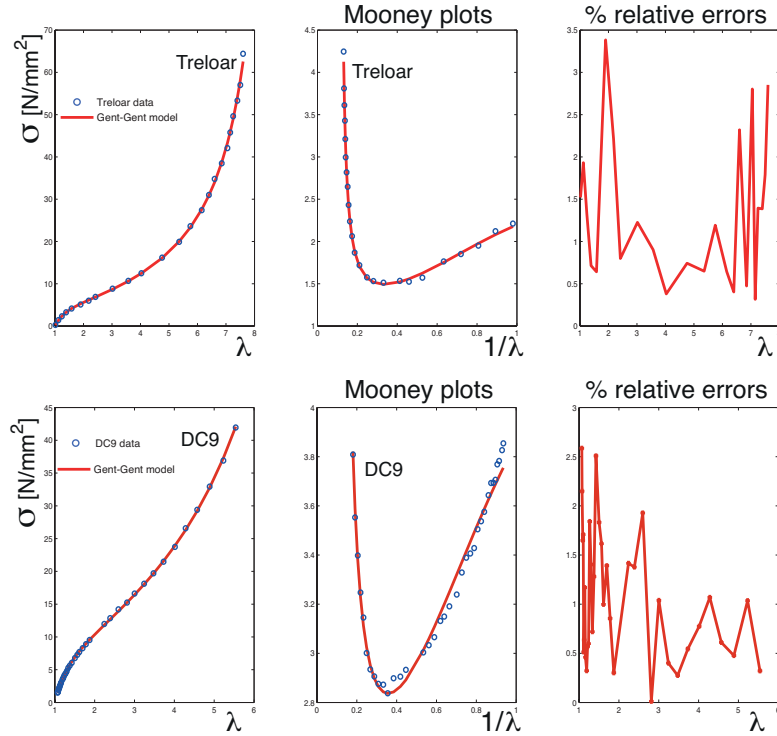


Figure 8: Non-linear least-square fitting over the entire range of experimental data with the three-parameter Gent-Gent model. Top: Treloar data; Bottom: DC9 data. The corresponding parameters are shown in Table 4.

In the literature, simple shear data are often inferred from a pure shear experiment, see for example Treloar (2005). Yeoh (1990) does present some simple shear data, obtained with a quadruple test. He observes that “These normal components of stress do not have much effect on the overall load/deformation behavior and are ignored.” However, we note there exists no protocol to measure normal stress components during a simple shear test, and therefore we cannot quantify and decide whether these stress quantities can indeed be neglected. In fact, normal stress effects (Poynting effect) can be observed directly in experiments, by drilling holes in the shearing plates and observing the bulging of the material, see examples by Rivlin (1947) or Destrade et al. (2015).

Now to draw meaning comparisons using the Mooney-Rivlin, Gent-Thomas and Carroll models (19), (20) and (21) we must stay in the small-to-moderate range of stretches, up to a maximal stretch of extension $\lambda_1 \simeq 2$, indicating that the material cannot be contracted to a stretch lower than $\lambda_2 = \lambda_1^{-1/2} = 0.71$. Because the amount of shear is related to the least stretch through

$K = \lambda_2^{-1} - \lambda_2$, we obtain a maximum of $K = 0.71$. In Figure 9(a) we plot the predictions in simple shear for Treloar's rubber, using the material constants of Table 2. Clearly all three models are in good accord, with the Carroll and Gent-Thomas models indicating a slight softening for shears $K \geq 0.5$.

Moving on the models (24), including a strain-hardening term to model the upturn, we now limit the simple shear predictions to the range $0 \leq K \leq 1.0$, as the upper bound reflects a tilting angle of 45° for the slanted faces, a clear *physical* limit for a realistic simple shear test. Figure 9(b) displays the comparison between each model, using the material parameters of Table 3, and again shows good agreement in the predictions.

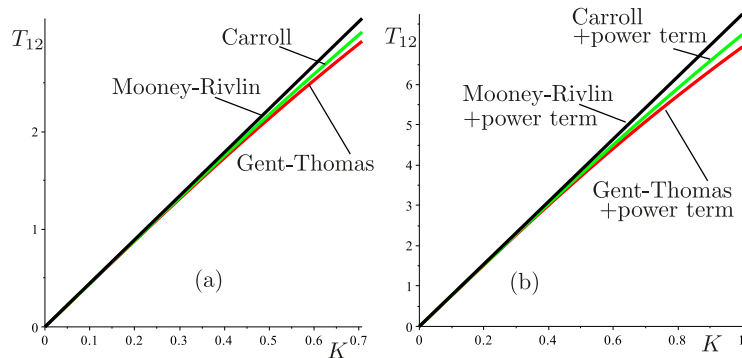


Figure 9: Predictions in simple shear of (a) the Mooney-Rivlin, Gent-Thomas and Carroll materials and of (b) the same materials augmented by a power-term to model strain-hardening, using Treloar's data.

These results confirm that the *robustness* already noticed in the fitting of simple extension data is conserved when considering a deformation with a completely different character (recall that simple shear is a plane deformation, with changing orientation of the principal axes with the deformation, in contrast to the three-dimensional uni-axial tension with conserved principal orientations).

Next we consider the following *rectilinear shear deformation*

$$x = X + h(Y), \quad y = Y, \quad z = Z, \quad (38)$$

for an unknown function h . This inhomogeneous deformation leads to a simple boundary value problem (BVP) which has to be solved numerically for each different model. The BVP is as follows: a slab is located in the region $-H \leq Y \leq H$, and its deformation is driven by a gradient of pressure in the X -direction, with $h(-H) = h(H) = 0$, see Ogden et al. (2004) for

details. The aim here is again to check whether the various models with material parameters listed in Tables 2 and 3 make comparable predictions of the deformation field. The answer is found in Figure 10, showing $h(Y)$ through the slab when $H = 1$, for increasing levels of pressure gradient: the variation between the different models is hardly noticeable, showing again the robustness of the methodical modelling presented in the paper. This result is in sharp contrast to the simulations conducted by Ogden et al. (2004) for the same BVP: there the same Ogden models, characterised by different values of the material parameters, gave the same close fitting to uni-axial tension and yet predicted different deformations.

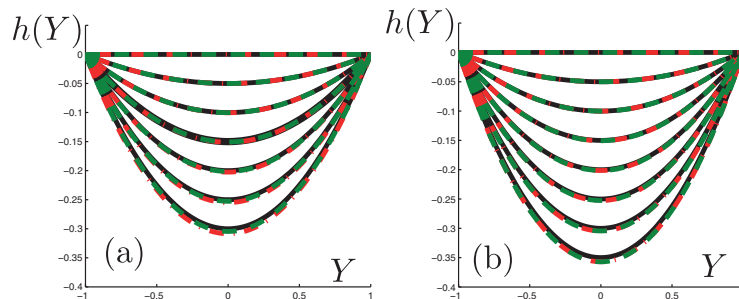


Figure 10: Predictions for the inhomogeneous rectilinear shear of (a) the Mooney-Rivlin (full black line), Gent-Thomas (dashed red line) and Carroll (dashed Green line) materials and of (b) the same materials augmented by a power-term to model strain-hardening, using Treloar’s data.

5 Conclusion and discussion

The fitting of constitutive parameters in the mathematical models of rubber-like materials is often considered to be a trivial task, although in fact this is not the case at all. Indeed more than 10 years ago, Ogden et al. (2004) had already pointed out how the fitting procedure is a very delicate aspect of the modelling procedure. Here we went one step further and proposed a possible solution to the main issues. Our solution is not a new form of the strain-energy; rather it is intrinsic to the theory of nonlinear elasticity and proves its robustness.

We used experimental data already published in literature to show that our method is quite general and does not rely too heavily on the quality of the experimental data to capture the salient features of the behavior of rubber. Clearly, it is possible to collect data in a more careful and uniform way for our treatment, for example by fixing a priori the range of extension

of interest and by fixing a uniform incremental step in the acquisition of the data for all the samples.

The starting point of our method was to delineate three ranges of deformations in the non-linear framework: the small-to-moderate range, the strain-hardening range (the zone of the upturn point in the Mooney plot), and the region of limiting-chain singularity. The aim of the procedure was to find a mathematical model able to fit the data within a reasonable error in part or all of the range. The main focus was more on the computational aspect of the fitting procedure than on the corresponding potential experimental issues. Using a step-by-step method, we eventually came to the conclusion that the theory of non-linear elasticity is a more robust theory than was previously thought.

We saw that minimising the relative errors of (14), as opposed to minimising the classical (absolute) residuals of (13), ensures consistency of the fitting procedure across the various measures of stress and strain.

We demonstrated quantitatively that for incompressible materials, the strain energy must depend on both principal invariants I_1 and I_2 . Moreover, we found that any standard linear combination of function of these two invariants fits well the data in the small-to-moderate range.

Then in order to model the upturn zone, we proposed an additional term to incorporate strain-stiffening effects. We also required full compatibility with the weakly non-linear theory of fourth-order elasticity. This compatibility is not a mathematical whim but is dictated by the generality of the response of rubber-like materials to large shear and large bending deformations. Again the resulting model provides a robust mathematical behaviour able to capture the data with low relative errors.

For the last step we needed to understand what is going on at very large deformations. This range of deformation has been studied in details in the last two decades and two reliable models have emerged: the Worm Like Chain model (Ogden et al. 2006) and the Freely Jointed Chain model, itself accurately modelled by the Gent model (Gent 1996, Puglisi and Saccomandi 2015). We proposed a practical way to investigate the mathematical behaviour of the vertical asymptote associated with the limiting-chain effects, and thus determine the order of the singularity for a given set of data. Hence we were able to confirm the insights coming from statistical mechanics computations on ideal macromolecular chains.

Finally, we showed that the three-parameter Gent-Gent model proposed by Pucci and Saccomandi (2002) is capable of fitting the entire deformation range with low relative error for both sets of experimental data studied. This versatility singles out the Gent-Gent strain energy density as a powerful model for all non-linear aspects of rubber-like behaviour (see also Ogden et

al. (2004), Pucci and Saccomandi (2002), Mangan and Destrade (2015)), although we note that the other five models investigated also performed well at the curve-fitting tasks, including the Carillo-Dobryin model proposed in 2011.

By deconstructing, decrypting and then recomposing all the puzzle of mathematical models for rubber-like materials, we provided evidence that the theory of non-linear elasticity can describe accurately uni-axial tension data with a strictly bounded error and a low number of unique parameters. The theory of non-linear elasticity is a basic, well-grounded theory of continuum mechanics. It is a mandatory passage required to explain the mechanical behaviour of many real-world materials. Therefore it was fundamental to confirm that this theory is not only mathematically well founded but also provides a robust description of experimental data, which is not contingent to the choice of a specific strain energy function, provided it satisfies some basic requirements and is adequate for (a) given regime(s). Using one of the other models proposed in the literature instead of the ones constructed here cannot change our main findings, because the heart of the modelling problem is independent on the functional form of the strain energy but relies instead on the methodology of fitting and on the way we read the data. This is essentially good news for the theory of nonlinear elasticity. Indeed if this theory was dependent on the choice of a given functional form, we would have to declare it a poor and restricted mathematical theory of mechanics.

Finally, because one of the most important elements of a computer simulation for deformable solid mechanics is the actual model of a material, our findings on the mathematical structure of the mathematical models for rubber-like materials is bound to have non-trivial consequences on their numerical implementation.

References

- Arruda, E. M. and M.C. Boyce, “A three-dimensional constitutive model for the large stretch behavior of rubber elastic materials,” *J. Mech. Phys.* **41**, 389–412 (1993).
- Ball, J. M. and R.D. James, “The Scientific Life and Influence of Clifford Ambrose Truesdell III,” *Arch. Rational Mech. Anal.* **161**, 1–26 (2002).
- Becker, G. W. and O. Kruger, “On the nonlinear biaxial stress-strain behavior of rubberlike polymers”. In *Deformation and Fracture of High Polymers* (Kausch, H. H., Hessel, J. A., Jaffee, R. I., Eds.) Plenum Press, New York (1972).

- Beda, T. “An approach for hyperelastic model-building and parameters estimation a review of constitutive models”. *Eur. Polym. J.* **50**, 97–108 (2014).
- Boyce, M. C. and E. M. Arruda, “Constitutive models of rubber elasticity: A review.” *Rubber Chem. Tech.* **73**, 504–523 (2000).
- Brown, R. *Physical testing of rubber*. Springer Science and Business Media (2006).
- Carroll, M. M. “A strain energy function for vulcanized rubber,” *J. Elast.* **103**, 173–187 (2011).
- Destrade, M., A. Goriely and G. Saccomandi, “Scalar evolution equations for shear waves in incompressible solids: A simple derivation of the Z, ZK, KZK, and KP equations,” *Proc. Roy. Soc. A* **467**, 1823–1834 (2011).
- Destrade, M., M.D. Gilchrist and J.G. Murphy, “Onset of non-linearity in the elastic bending of blocks,” *ASME J. Appl. Mech.* **77**, 061015 (2010).
- Destrade, M., J. G. Murphy and G. Saccomandi, “Simple shear is not so simple,” *Int. J. Non-Linear Mech.* **47**, 210–214 (2012).
- Destrade, M., M.D. Gilchrist, J.G. Murphy, B. Rashid and G. Saccomandi, “Extreme softness of brain matter in simple shear,” *Int. J. Non-Linear Mech.* **75**, 54–58 (2015).
- Destrade, M. and R.W. Ogden, “On the third- and fourth-order constants of incompressible isotropic elasticity,” *J. Acoust. Soc. Am.* **128**, 3334–3343 (2010).
- De Tommasi, D., G. Puglisi and G. Saccomandi, “Multiscale mechanics of macromolecular materials with unfolding domains,” *J. Mech. Phys. Solids* **78**, 154–172 (2015).
- Dobrynin, A. V. and J.-M. Y. Carrillo, “Universality in nonlinear elasticity of biological and polymeric networks and gels,” *Macromol.* **44**, 140–146 (2011).
- Flory, P. *Statistical Mechanics of Chain Molecules*, Hanser Publisher, Munich (1989).
- Gent, A. N. “A new constitutive relation for rubber,” *Rubber Chem. Technol.* **69**, 59–61 (1996).

- Gent, A. N. and A.G. Thomas, “Forms for the stored (strain) energy function for vulcanized rubber,” *J. Polymer Sc.* **28**, 625–628 (1958).
- Golub, G. H. and V. Pereyra, “Separable nonlinear least squares: The variable projection method and its applications,” *Inv. Probl.* **19**, 1–26 (2003).
- Hamilton, M. F., Y.A. Ilinskii and E.A. Zabolotskaya, “Separation of compressibility and shear deformation in the elastic energy density,” *J. Acoust. Soc. Am.* **116**, 41–44 (2004).
- Horgan, C. O., and G. Saccomandi. ”Finite thermoelasticity with limiting chain extensibility.” *J. Mech. Phys. Solids* **51**, 1127–1146 (2003).
- Kearsley, E. A. “Note: Strain invariants expressed as average stretches,” *J. Rheol.* **33**, 757–760 (1989).
- Klingbeil, W. W. and R.T. Shield, “Some numerical investigations on empirical strain-energy functions in the large axisymmetric extensions of rubber membranes,” *J. Appl. Math. Phys.* **15**, 608–629 (1964).
- Lopez-Pamies, O. “A new I_1 -based hyperelastic model for rubber elastic materials,” *Comptes Rend. Méca.* **338**, 3–11 (2010).
- Mangan, R. and M. Destrade. “Gent models for the inflation of spherical balloons,” *Int. J. Non-Linear Mech.* **68**, 52–58 (2015).
- Marckmann, G. and E. Verron. “Comparison of hyperelastic models for rubber-like materials,” *Rubber Chem. Tech.* **79**, 835–858 (2006).
- Mooney, M. “A theory of large elastic deformation,” *J. Appl. Phys.* **11**, 582–592 (1940).
- Motulsky, H. and A. Christopoulos, *Fitting Models to Biological Data Using Linear and Nonlinear Regression: A Practical Guide to Curve Fitting*, University Press, Oxford (2004).
- Norris, A. N. “Finite-amplitude waves in solids,” In *Nonlinear Acoustics*, Eds M. F. Hamilton & D. T. Blackstock, Academic Press, London (1998).
- Ogden, R. W. “On isotropic tensors and elastic moduli,” *Proc. Camb. Phil. Soc.* **75**, 427–436 (1974).
- Ogden, R. W. *Non-Linear Elastic Deformations*, Ellis Horwood Ltd., West Sussex (1984).

- Ogden, R. W., G. Saccomandi and I. Sgura, “Fitting hyperelastic models to experimental data,” *Comput. Mech.* **34**, 484–502 (2004).
- Ogden, R. W., G. Saccomandi and I. Sgura, “On worm-like chain models within the three-dimensional continuum mechanics framework,” *Proc. R. Soc. A* **462**, 749–768 (2006).
- O’Leary, D. P. and B.W. Rust, “Variable projection for nonlinear least squares problems,” *Comp. Optim. Appl.* **54**, 579–593 (2013).
- Pincus, P. “Excluded volume effects and stretched polymer chains,” *Macromol.* **9**, 386–388 (1976).
- Pucci, E. and G. Saccomandi, “A note on the Gent model for rubber-like materials,” *Rubber Chem. Technol.* **75**, 839–851 (2002).
- Puglisi, G. and G. Saccomandi, “The Gent model for rubber-like materials: An appraisal for an ingenious and simple idea,” *Int. J. Non-Linear Mech.* **68**, 17–24 (2015).
- Puglisi, G., and G. Saccomandi. ”Multi-scale modelling of rubber-like materials and soft tissues: an appraisal.” *Proc. R. Soc. A.* **472**, # 20160060 (2016).
- Saccomandi, G. “Some mechanical problems from rubber mechanics, block copolymers, DNA mechanics and biomechanics,” in: R.W. Ogden and L. Dorfmann (Eds), *CISM Lecture Notes on Nonlinear Mechanics of Soft Fibrous Materials*, Springer, Vienna (2015).
- Rivlin, R.S. “Torsion of a rubber cylinder,” *J. Appl. Phys.* **18**, 444–449 (1947).
- Rivlin, R.S. *Collected Papers of R.S. Rivlin*, Springer, New York (1996).
- Rubinstein, M. and R.H. Colby, *Polymer Physics*, Oxford University Press, New York (2003).
- Rubinstein, M. and S. Panyukov, “Elasticity of polymer networks,” *Macromol.* **35**, 6670–6686 (2002).
- Toan, N. M. and D. Thirumalai, “Theory of biopolymer stretching at high forces,” *Macromol.* **43**, 4394–4400 (2010).
- Treloar, L. R. G. *The Physics of Rubber Elasticity*, Clarendon Press: Oxford (2005).

Truesdell, C. “Das ungelöste Hauptproblem der endlichen Elastizitätstheorie”, ZAMM **36**, 97–103 (1956).

Yeoh, O. H. “Characterisation of elastic properties of carbon-filled rubber vulcanizates,” Rubber Chem. Technol. **63**, 792–805 (1990).